Journal Name

ARTICLE

Impact of Macromolecular Crowding on RNA/Spermine Complex Coacervation and Oligonucleotide Compartmentalization

Received 00th January 20xx,
Accepted 00th January 20xx

DOI: 10.1039/x0xx00000x

www.rsc.org/

A. M. Marianelli,[a] B. M. Miller[a] and C. D. Keating*[a]

We report the effect of neutral macromolecular crowders poly(ethylene glycol) (PEG) (8 kDa) and Ficoll (70 kDa) on liquid liquid phase separation in a polyuridylic acid (polyU)/spermine complex coacervate system. The addition of PEG decreased both the amount of spermine required for phase separation and the coacervation temperature (T_C). We interpret these effects on phase behavior as arising due to excluded volume and preferential interactions on both the secondary structure/condensation of spermine-associated polyU molecules and on the association of soluble polyU/spermine polyelectrolyte complexes to form coacervate droplets. Examination of coacervates formed in the presence of fluorescently-labeled PEG or Ficoll crowders indicated that Ficoll is accumulated while PEG is excluded from the coacervate phase, which provides further insight into the differences in phase behavior. Crowding agents impact distribution of a biomolecular solute: partitioning of a fluorescently-labeled U15 RNA oligomer into the polyU/spermine coacervates was increased approximately two-fold by 20 wt.% Ficoll 70 kDa and by more than two orders of magnitude by 20 wt.% PEG 8 kDa. The volume of the coacervate phase decreased in the presence of crowder relative to a dilute buffer solution. These findings indicate that potential impacts of macromolecular crowding on phase behavior and solute partitioning should be considered in model systems for intracellular membraneless organelles.

Introduction

A number of non-membranous organelles, such as nucleoli[1] and P granules,[2] are thought to form by liquid-liquid phase separation (LLPS).[3-11] These protein- and RNA-rich intracellular condensates appear to be crucial for cellular function, playing roles in signaling, sequestration, and spatiotemporal reaction control.[11] LLPS is a relatively general demixing phenomenon that occurs in solutions containing macromolecules; different types of molecular interactions (e.g., poor macromolecule solvation, ion pairing, and/or specific biomolecular binding) can be important depending on the system. Ion-pairing interactions appear to play important roles in the formation of several membraneless organelles,[3, 7-9, 12] suggesting that a type of LLPS referred to as complex coacervation could provide useful model systems. Complex coacervation occurs in solutions of oppositely charged macromolecules and results in the formation of a dense polyelectrolyte-rich phase (termed the coacervate phase) and a dilute supernatant phase. Complex coacervation can occur with a wide range of polyelectrolyte pairs,[13-15] and is sensitive to changes in the solution environment such as salt concentration,[16, 17] pH,[13, 18] temperature,[14, 15] and post-translational modifications like phosphorylation.[19] This tunability mimics an important aspect of intracellular phase separation: the ability to modulate phase behavior in response to biological stimuli. Purified solutions of key protein components of membraneless organelles have been shown to undergo environment-dependent LLPS. P granules found in the embryos of *C. elegans* have been shown to regulate their assembly and disassembly by phosphorylation of serine-rich proteins.[20] Temperature has been shown to modulate phase separation of intracellular droplets containing the intrinsically disordered protein (IDP) Ddx4,[3] as well as stress granules composed of the ALS-related protein FUS.[21]

Dense polyelectrolyte-rich coacervate droplets mimic important aspects of intracellular phase separation, but the accompanying dilute supernatant phase does not accurately model any cellular compartments. The cellular environment contains up to 300-400 mg/mL of macromolecules, which results in a macromolecularly crowded solution that does not behave according to thermodynamic ideality.[22, 23] Crowding impacts molecules in solution through both volume exclusion, the reduction of volume available to molecules due to the volume occupied by other macromolecules, and nonspecific chemical effects, preferential or repulsive interactions between molecules.[24] Volume exclusion can lead to increased effective concentrations of solutes, sometimes by orders of magnitude, which could facilitate phase separation at lower polyelectrolyte concentrations.[23, 25] Early crowding studies showed that the activity coefficient of hemoglobin (Hb) increased

[a] *Department of Chemistry, Pennsylvania State University, University Park, Pennsylvania 16802, United States. E-mail: keating@chem.psu.edu*

† Footnotes relating to the title and/or authors should appear here.

Electronic Supplementary Information (ESI) available: Plots showing residuals for turbidity fits, U15 RNA partitioning vs. crowder concentration, and coacervate phase volume vs. crowder concentration, and calculations for volume determination. See DOI: 10.1039/x0xx00000x

tenfold as the concentration of Hb increased from 200 mg/mL to 300 mg/mL, near the physiological Hb content of red blood cells (350 mg/mL).[26, 27] Taylor and coworkers,[9] as well as Lin et. al.,[28] have observed that crowding increased the propensity for formation of liquid droplets with RNA and protein components by decreasing the amount of protein required for phase separation. Crowding has also been shown to support LLPS of the Alzheimer-related protein Tau.[29] PEG has been shown to increase the upper critical solution temperature (UCST, temperature above which phase separation no longer occurs) for a number of systems, including various eye lens proteins[30, 31] and IgG antibody solutions,[32] promoting persistence of phase separation. In these cases, PEG-induced LLPS is thought to occur due to depletion forces as a result of inter-protein attractive interactions.[30, 33, 34] Volume exclusion alone is predicted to favor more compact structures, thus favoring protein folding, RNA/DNA structure, associative interactions, and aggregation.[25, 35-42] Repulsive chemical interactions can enhance the effects caused by volume exclusion, while preferential interactions can minimize or compensate for the volume exclusion effects depending on the magnitude of the interactions.[43] Associative LLPS described by complex coacervation, where extended rather than compact conformations favor phase separation due to the necessity for ion pairing between separate molecules, may behave differently in the presence of crowding agents than LLPS through protein self-association driven by poor solvation or specific biorecognition motifs.[11, 44-46] The functional properties of coacervate droplets (e.g. ability to interact with/colocalize crowders and biomolecules) are also likely to be affected by crowding, and have not, to our knowledge, been previously explored for any coacervate system. These considerations highlight the importance of determining the impact of high macromolecule content on experimental model systems for biology.

In contrast to protein-based phase separation, the effect of macromolecular crowding on RNA-based coacervation has not been explored. In vivo, membraneless organelles often contain both proteins and RNA.[1, 2, 4, 6] These structures are important for RNA processing and contain proteins with RNA-binding motifs, so it follows that RNA could have an important role in their formation.[45] Indeed, RNA has been shown to promote phase separation in many scenarios, including the formation of *C. elegans* nucleoli,[4] ribonucleoprotein (RNP) granules,[6] paraspeckles,[47] and stress granules.[9] Unlike many intrinsically disordered proteins associated with membraneless organelles, nucleic acids do not self-associate to phase separate in the absence of multivalent counterions. In the presence of polycations, nucleic acids can form soluble complexes as well as solid (precipitate) or liquid (coacervate) condensed phases.[48-53] Polyamines are present in the intracellular environment,[54, 55] and often associated with RNA.[54]

Here, we investigated the impact of macromolecular crowding on coacervation of RNA and spermine to generate a more accurate model for membraneless organelles, which are surrounded by the crowded intracellular milieu rather than by a dilute buffer solution. (Figure 1). We chose polyuridylic acid (polyU, MW 600 – 1,000 kDa), a long, low complexity RNA having minimal secondary structure, as our polyanion and the naturally occurring polyamine, spermine, as our cation. Coacervation in the polyU/spermine system[14, 56] occurs predominantly via an ion pairing (complex coacervation) mechanism. PEG and Ficoll, the crowding molecules utilized here, are neutral macromolecules that are commonly used to mimic intracellular crowding conditions.[9, 23, 25, 57, 58] We found that PEG promotes polyU/spermine complex coacervation. Although PEG was excluded from coacervate droplets and Ficoll was accumulated within them, both PEG and Ficoll improved partitioning of an RNA oligonucleotide and decreased the overall coacervate phase volume. This work highlights the importance of considering macromolecular crowding when generating experimental model systems, as it can have significant impacts on the phase behavior of complex coacervation.

Materials and methods

Materials

Polyuridylic acid (polyU) potassium salt (MW 600 – 1,000 kDa), spermine tetrahydrochloride, HEPES, HEPES sodium salt, magnesium chloride hexahydrate ($MgCl_2$•$6H_2O$), poly(ethylene glycol) (PEG) (MW 7-9 kDa), Ficoll (MW 60 – 80 kDa), and Ficoll-tetramethylrhodamine isothiocyanate (TRITC) (MW 30 – 50 kDa) were purchased from Sigma Aldrich (St. Louis, MO). Ethylene glycol (EG) was obtained from Amresco (Solon, OH). Dextran (MW 9 – 11 kDa) was purchased from CedarLane Labs (Ontario, Canada). Sucrose and nuclease-free water were purchased from Thermo Fisher Scientific (Waltham, MA). Fluorescently-labeled PEG, mPEG-

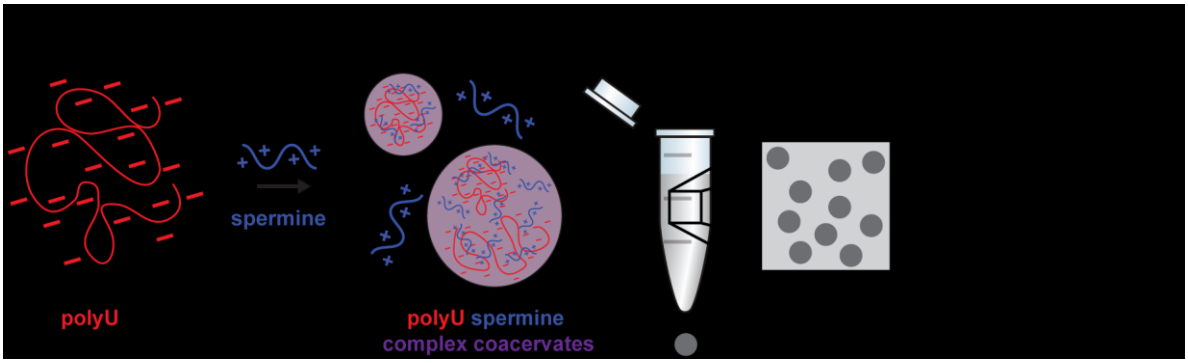

Figure 1: Schematic view depicting the objective of this research. Complex coacervation **(left)** is a charge-based type of liquid liquid phase separation resulting in a dense polyelectrolyte-rich coacervate phase that models membraneless organelles and a dilute supernatant phase that does not mimic the cellular environment. The goal of this work is to elucidate the impact of macromolecular crowding **(center)** on complex coacervation to generate more accurate experimental model systems of intracellular organization.

fluorescein isothiocyanate (FITC) (MW 4 – 6 kDa) was obtained from Creative PEGWorks (Winston Salem, NC). The fluorescently-labeled oligonucleotide, U15 RNA, was 5'-labeled with Alexa Fluor 647 (NHS ester) and purchased from Integrated DNA Technologies (Coralville, IA). Secure-seal one well spacers (9 mm diameter, 0.12 mm deep) from Life Technologies (Carlsbad, CA) or silicone spacers (9 mm diameter, 2 mm deep) from Electron Microscopy Sciences (Hatfield, PA) and micro cover glasses (no. 1.5, 24 x 30 mm) from VWR (West Chester, PA) were used for optical microscopy imaging. Glass slides were silanized (using N-(triethoxysilylpropyl)-o-polyethylene oxide urethane) prior to use as previously described to render the surface hydrophobic and prevent coacervate droplets from exhibiting non-spherical geometries.[59] Chemicals were used as received.

Instrumentation

Turbidity measurements were taken using either Agilent 8453 diode-array UV-visible spectrometers with Agilent ChemStation software coupled with Agilent 89090A Peltier temperature controllers or an OLIS 8453 diode-array UV-visible spectrometer with OLIS interface and SpectralWorks software coupled with an OLIS linear six-position Peltier cell holder. Confocal images were taken using a Leica TCS SPS laser scanning confocal inverted microscope (LSCM) with Leica LAS AF software, a 63x oil objective, and an Instec TSA021 temperature-controlled stage. Bulk fluorescence measurements were made using a Fluorolog 3-21 fluorimeter with FluorEssence software and a Wavelength Electronics temperature controller. Fluorescence quantification of coacervate images was completed in ImageJ, and graphing was done in IgorPro Version 6.37 software.

Coacervate Preparation

A 1 wt.% stock solution of polyU was prepared in nuclease-free water and stored in multiple aliquots at -20 °C. Final concentrations of polyU ranged from 0.005 wt.% (~0.05 – 0.08 μM) to 0.05 wt.% (~0.5 – 0.8 μM) polyU. Multiple stock solutions (0.1 – 10 wt.%) of spermine were prepared in deionized water and stored at 5 °C. Final concentrations of spermine ranged from 0.0005 wt.% (14 μM) to 0.05 wt.% (1440 μM). Crowder (PEG and Ficoll) and small molecule analog (EG and sucrose) stock solutions were prepared at 25 wt.% in deionized water and stored at 5 °C. The Alexa 647-U15 RNA stock solution was prepared at 100 μM in nuclease-free water and stored at 5 °C. Coacervates were prepared in a 5 mM HEPES (pH 7.4), 1 mM $MgCl_2$ buffer. Stock solutions were added in the following order for preparation of each sample: deionized water, HEPES, $MgCl_2$, crowder/small molecule, polyU, spermine, oligonucleotide (for partitioning experiments). Samples were mixed via gentle pipetting in between the addition of each stock solution.

Characterization of Coacervate Formation

The amount of spermine required for coacervation with 0.05 wt.% polyU in a 5 mM HEPES (pH 7.4), 1 mM $MgCl_2$ buffer at 37 °C was determined using UV-visible spectroscopy by measuring the sample absorbance/transmittance at 500 nm and converting to turbidity (T_{500}, turbidity = 100 - % transmittance). Samples were incubated at 37 °C for 5 min prior to measurement and held at 37 °C during measurement. The phase transition temperature (or coacervation temperature, T_C) of polyU/spermine coacervates was also determined using UV-visible spectroscopy as described above. The temperature was ramped from 5 – 40 °C in 0.5 °C increments, incubating at each temperature for 12 sec. PolyU structure was probed using UV-visible spectroscopy as well, by measuring the sample absorbance/transmittance at 260 nm and converting to normalized absorbance (A_{260}). Normalization was completed using the highest absorbance value in each temperature range. The data were plotted using IgorPro Version 6.37 graphing software.

Curve Fitting

Due to the steepness of the transition to maximal turbidity, standard deviations from three experimental trials are higher in this region of the plot. In order to take standard deviation into account and avoid user bias when determining the transition midpoint, curve fitting was used to describe the shape of the dataset. Sample turbidity vs. wt.% spermine and sample turbidity vs. temperature data were fit using the four-parameter logistic nonlinear regression model (also known as the Hill equation or the variable slope sigmoidal equation) (eq 1), in IgorPro Version 6.37 software. Although this equation was developed to describe biomolecule binding curves, data unrelated to biomolecule binding but still assuming a sigmoidal shape are well described by the equation.[60-63] Residuals (provided in ESI, Figure S1 and S3) represent error in the fit and are weighted by the standard deviation of triplicate measurements. The calculated x values required to achieve 50% maximal turbidity represent the amount of spermine required for phase separation and the coacervation temperature (T_C), respectively, and take into account the error from triplicate measurements of sample turbidity.

Eq 1 $$f(x) = base + \frac{(max - base)}{1 + \left[\frac{xhalf}{x}\right]^{rate}}$$

Coacervate Imaging

Confocal microscopy images were collected with an excitation at 488 nm for FITC-labeled PEG, 543 nm for TRITC-labeled Ficoll, and 633 nm for Alexa 647-labeled U15 RNA. The temperature stage was held at 37 °C to maintain phase separation within the sample. Fluorescent U15 RNA concentration inside droplets was calculated using a calibration curve of the fluorescently-labeled oligonucleotide in buffer.

Bulk Fluorescence Measurements

Bulk fluorescence measurements for determining the Alexa 647-U15 RNA concentration in the supernatant phase were made using an excitation of 633 nm. The temperature was held at 37 °C. Coacervate samples were prepared as described above, incubated at 37 °C for 30 minutes, then centrifuged (at 37 °C and 13,200 rpm) to form a single coalesced coacervate phase at the bottom of the tube. The supernatant phase was then removed for bulk fluorescence measurements. Fluorescent U15 RNA concentration was determined from calibration curves of the fluorescently-labeled oligonucleotide in buffer.

Results and discussion

Macromolecular crowders might be expected to impact several aspects of complex coacervation in the polyU/spermine system.

These include: (i) polyU conformation, (ii) formation of polyU/spermine soluble complexes, and (iii) complex coacervation to form polyU/spermine-rich droplets.[14, 64, 65] We used the common neutral crowding agents PEG (molecular weight (MW) 8 kDa) and Ficoll (70 kDa) and their small molecule analogs, EG and sucrose, to probe the impact of macromolecular crowding on the formation and properties of polyU/spermine coacervates.

Previous work in our lab has established the salt, polyamine, and temperature-dependent phase behavior of complex coacervation between polyU and spermine, as well as its ability to compartmentalize peptides and oligonucleotides.[14] Phase separation was shown to occur between polyU and spermine across a range of charge ratios from 0.7 (+/-) to 100, and coacervate droplets were stable at salt concentrations of up to 200 mM NaCl. The coacervate system also exhibited lower critical solution temperature (LCST) behavior, existing as a single phase below ambient temperature (~22 °C), and undergoing phase separation upon heating. The LCST behavior was hypothesized to occur as a result of a loss in polyU secondary structure and adoption of a random coil, rendering more of polyU's negative charges available to interact with the cationic spermine.[14] Here, we first evaluate the effect of crowders on phase separation, then explore their distribution between the coacervate and supernatant phases, and finally quantify the impact of crowders on the accumulation of a labeled RNA oligonucleotide within the coacervates.

Spermine Content Required for Coacervation

We first evaluated the amount of spermine, and thus the charge balance, required for polyU/spermine coacervation of a fixed amount of polyU RNA (Figure 2). Sample turbidity was used to identify phase separation. In the absence of crowder and with constant polyU (0.05 wt.%), coacervation occurred with a minimum of 0.0071 wt.% spermine (a +/- charge ratio of 0.8), which is consistent with previous results.[14] Increasing amounts of PEG 8 kDa led to a significant decrease in the spermine (0.0051 wt.%, charge ratio: 0.58 for 20 wt.% PEG) required to induce coacervation (Figure 2A). Increasing the amount of EG exhibited a trend similar in direction but smaller in magnitude (0.0056 wt.%, charge ratio: 0.64 for 20 wt.% EG) (Figure 2B). In contrast, neither Ficoll 70 kDa nor sucrose appreciably impacted the amount of spermine required for phase separation (Figure 2C-D). To determine whether the differences between crowders was related to molecular weight[66-68] or chemistry, we also tested dextran 10 kDa, another polysaccharide structurally similar to Ficoll but with a molecular weight close to that of PEG. Dextran 10 kDa did not have as significant an impact on the amount of spermine required for coacervation as did PEG 8 kDa (Figure S2), suggesting that size of the crowding molecule is not primarily responsible for the differing effects observed here. The similar impacts observed for PEG 8 kDa and EG further suggest that the trend is not entirely due to excluded volume.[39]

Beyond excluded volume effects, crowders and cosolutes can influence the conformation and association state of nucleic acids by changes in water activity or chemical interactions with functional groups on the macromolecule of interest; together these effects can be termed chemical effects or preferential interactions.[69, 70] For example, PEGs with MWs lower than 6 kDa and EG have been shown to destabilize RNA hairpins as a result of hydrophobic interactions between (P)EG and RNA nucleobases.[71] Knowles et. al. found that EG and other small, non-crowding PEGs (MW<200 Da) destabilized DNA hairpins and duplexes due to preferential chemical interactions between EG and the DNA nucleobases exposed during melting.[39] Both PEG and EG can experience attractive chemical interactions with the polyU nucleobases, which could favor an extended polyU structure, allowing spermine more access to the negatively charged polyU. However, preferential interactions between PEGs and DNA have been shown to decrease with increasing PEG MW, as a larger percent of the PEG segments become buried within the flexible PEG coil, shielding them from DNA interactions.[39] Crowding has been shown to decrease the water activity in solution,[72, 73] with PEG[74] depressing water activity to a much greater extent than Ficoll.[71, 75] This decrease in water activity can favor the less-hydrated unfolded states of nucleic acids.[73, 76] EG has also been shown to significantly decrease water activity.[71] Neither Ficoll nor sucrose impact water activity with the same magnitude as PEG and EG,[71] nor are they likely to exhibit the same types of preferential interactions with the polyU RNA. Our data are consistent with the hypothesis that preferential interactions with PEG and EG destabilize the secondary structure of polyU, facilitating interactions between polyU and spermine at lower spermine concentrations, thus promoting first polyU/spermine soluble complexation followed by complex coacervation.

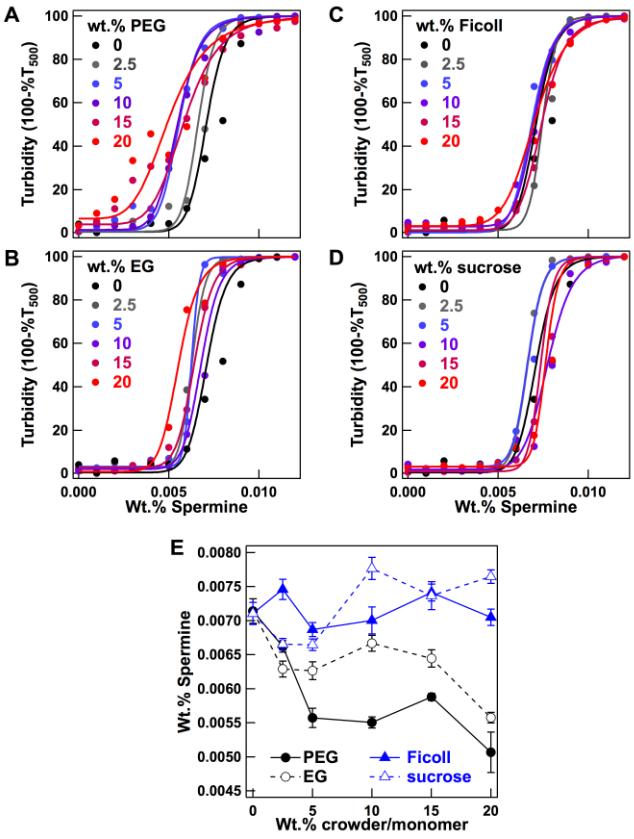

Figure 2: Effect of crowders and their small molecule analogs on the amount of spermine required to induce coacervation. Fitting of turbidity (to eq 1) as a function of

wt.% spermine for 0.05 wt.% polyU, parametric in wt.% **(A)** PEG, **(B)** EG, **(C)** Ficoll, and **(D)** sucrose. Data points represent the average of triplicate measurements. **(E)** Spermine required to induce coacervation as a function of wt.% probe molecule. Turbidity midpoints were calculated from fits as described in Methods. Both PEG and EG decrease the amount of spermine required for phase separation, but the effect of PEG is more dramatic than that of EG. Neither Ficoll nor sucrose has a significant impact on spermine required for coacervation. Error bars represent standard deviation calculated from the fits in **(A-D)**. Residuals representing errors in fit can be found in Figure S1.

Temperature-Dependence of PolyU/Spermine Coacervation

The polyU/spermine coacervate system exhibits temperature-dependent phase behavior, existing as a single phase below ambient temperature (~22 °C) in the absence of crowders, and undergoing phase separation at higher temperatures. The effect of crowding on this temperature-dependent behavior was investigated by measuring sample turbidity as a function of temperature in the presence of varying amounts of crowding molecules and their small molecule analogs.

Above 2.5 wt.% PEG, coacervation occurred at temperatures as low as 5 °C, but still exhibited slight transitions to maximum phase separation (Figure 3A). These data suggest that PEG promotes polyU/spermine coacervation at low temperatures, but upon heating, phase separation occurs to a greater degree (i.e. the quantity or size of coacervate droplets increases). In such a case, a number of factors, some temperature-sensitive, are likely impacting polyU/spermine phase behavior. Crowding typically favors associative or condensation reactions, as a result of volume exclusion, so condensation of soluble polyU/spermine complexes into complex coacervate droplets could also be supported by volume exclusion effects. These results are consistent with the hypothesis that PEG crowding increases the effective concentrations of spermine and polyU and exhibits preferential interactions that favor the unstructured polyU. However, the negligible impact of Ficoll, EG, and sucrose on the T_C (Figure 3B-D), is somewhat surprising, as one might expect to see similar impacts with smaller magnitude for both Ficoll (excluded volume) and EG (preferential interactions). To better understand these results, we next investigated the effect of the crowders and cosolutes on polyU secondary structure.

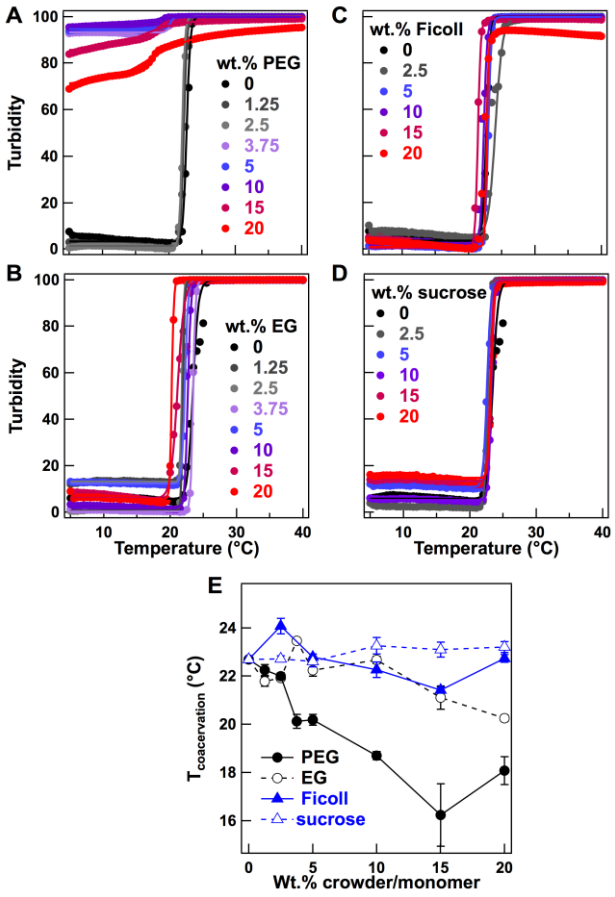

Figure 3: Effect of crowders and their small molecule analogs on the coacervation temperature (T_C) of polyU/spermine. Fitting of turbidity (to eq 1) as a function of temperature for 0.05 wt.% polyU/0.01 wt.% spermine, parametric in wt.% **(A)** PEG, **(B)** EG, **(C)** Ficoll, and **(D)** sucrose. Data points represent the average of triplicate measurements. **(E)** Coacervation temperature as a function of wt.% probe molecule. Turbidity midpoints were calculated from fits as described in Methods. PEG dramatically decreases the T_C, while Ficoll, EG, and sucrose have a negligible impact on T_C. Error bars represent standard deviation calculated from the fits in **(A-D)**. Residuals representing errors in fit can be found in Figure S3.

Secondary Structure of PolyU

In the absence of crowders, the LCST behavior exhibited by polyU/spermine occurred at the same temperature as the loss in (spermine-stabilized)[77] polyU secondary structure, suggesting that loss of polyU structure was required for phase separation.[14] PolyU melt experiments in the presence and absence of PEG, EG, Ficoll, and sucrose were completed to probe the impact of crowding and preferential interactions on polyU secondary structure, specifically base-stacking and hydrogen bonding. Hypochromicity, a decrease in absorbance at 260 nm, results from base stacking and is indicative of polynucleotide structure.[78, 79] Early work found that polyU, previously thought to have no appreciable ordered structure, exhibited both hypochromicity and an increase in optical rotation at temperatures below 10 °C, indicative of an ordered, helical structure.[80, 81] At low temperatures, polyU has been hypothesized to adopt a hairpin-like structure consisting of U-U hydrogen bonding.[80] The presence of polyamines, including spermine, has been shown to stabilize this structure, shifting the change in absorbance and optical rotation indicative of a loss in structure to

higher temperatures.[77] Our results suggest that the secondary structure of polyU changes in the presence of increasing amounts of crowders, but not in the presence of their small molecule analogs (Figure 4). Increasing amounts of crowder resulted in a decrease in the temperature at which polyU loses its secondary structure (T_m), indicative of a destabilization of base-stacking interactions. For PEG 8 kDa at 15 and 20 wt.%, the change in T_m (Figure 4A) appears to correlate with the inflection points in the temperature-dependent turbidity data at high PEG concentration (Figure 3A), suggesting that although loss of polyU structure was not necessary for phase separation in the presence of PEG, its occurrence nonetheless favors coacervation.

The initial A_{260} at low temperatures also increased above 10-15 wt.% PEG or Ficoll, suggesting that at temperatures as low as 5 °C, polyU has already lost some of its (spermine-stabilized)[14, 77] secondary structure. PEG and Ficoll thus appear to interfere with spermine's stabilization of polyU base-stacking. The transition from base-stacking secondary structure to a random coil exposes more negative charges on polyU that can interact with the cationic spermine, promoting coacervation at lower temperatures and spermine concentrations. The lack of impact on polyU melt behavior from the non-crowding probe molecules (EG and sucrose) suggests that volume exclusion, as opposed to nonspecific chemical interactions, is the driving force behind the observed decrease in T_C illustrated in Figure 3. It is interesting to note that PEG and Ficoll affect polyU's transition from secondary structure to random coil in similar ways, despite their significantly different impact on the T_C of polyU/spermine coacervation.

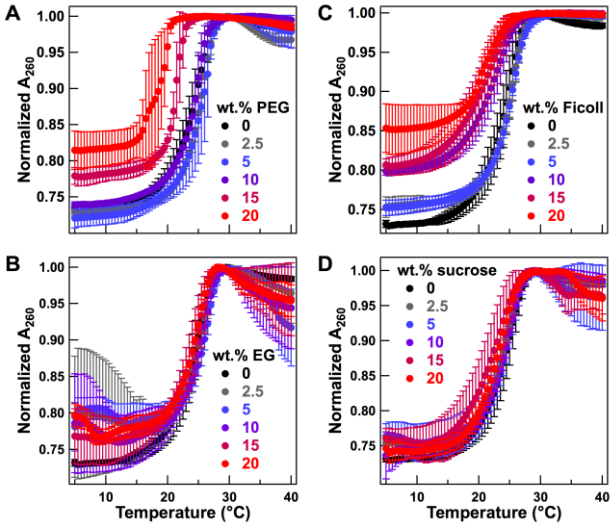

Figure 4: Normalized absorbance at 260 nm (A_{260}) as a function of temperature for 0.005 wt.% polyU/0.0005 wt.% spermine parametric in **(A)** PEG, **(B)** EG, **(C)** Ficoll, and **(D)** sucrose. Error bars represent standard deviation between triplicate measurements. Absorbance values are normalized to the highest absorbance measurement within each experiment. As the amounts of both PEG and Ficoll increase, the T_m decreases and the initial A_{260} increases. Neither EG nor sucrose significantly impact the T_m or initial A_{260}.

Additional polyU melt experiments were conducted in the absence of spermine with varying crowder/small molecule content to probe the potential impact of crowding on polyU structure alone (Figure 5). An increase in PEG shifted the T_m to higher temperatures, suggesting PEG stabilizes polyU secondary structure in the absence of spermine. This is in agreement with the prediction that volume exclusion favors folded, compact states, as well as experimental and theoretical evidence that nucleic acid structure is stabilized by macromolecular crowding.[25, 39, 48, 82, 83] The negligible impact of the small molecules EG and sucrose on polyU structure in the absence of spermine, specifically for EG, indicate important differences between PEG 8 kDa and the other molecules in their excluded volume and/or preferential interactions. Taken together, the results from Figures 4 and 5 show that coacervation in the presence of crowders cannot be understood solely on the basis of how crowders impact polyU secondary structure.

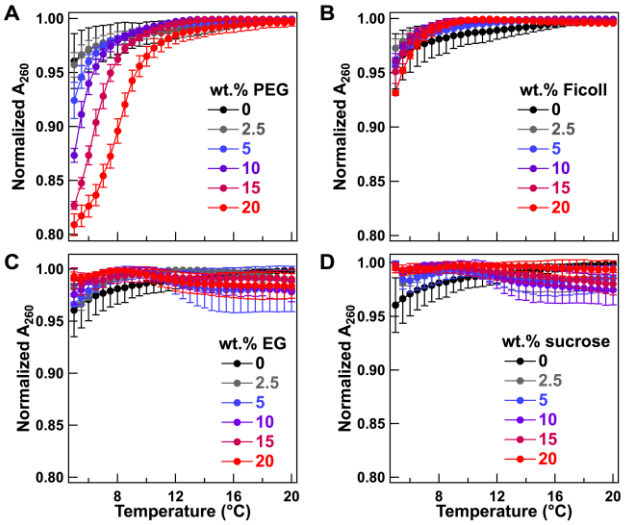

Figure 5: Normalized absorbance at 260 nm (A_{260}) as a function of temperature for 0.005 wt.% polyU with no spermine, parametric in **(A)** PEG, **(B)** EG, **(C)** Ficoll, and **(D)** sucrose. Error bars represent standard deviation between triplicate measurements. Absorbance values are normalized to the highest absorbance measurement within each experiment. As the amount of PEG increases, the T_m increases. Neither Ficoll, EG, nor sucrose significantly impact the normalized A_{260}.

Crowder and Oligonucleotide Partitioning

A number of membraneless organelles and in vitro liquid droplets composed of RNA and intrinsically disordered proteins have been shown to concentrate and compartmentalize biomolecules, including oligonucleotides.[3, 84-87] This capability is considered central to their function.[11, 88, 89] Therefore, it is important to probe the potential impact of a crowded environment on biomolecule partitioning. Compartmentalization of fluorescently labeled PEG, Ficoll, and the 15-nt oligonucleotide U15 RNA was investigated using a combination of confocal fluorescence microscopy and bulk fluorescence measurements. We found that FITC-PEG 5 kDa was excluded from the coacervate phase to an increasing degree as the amount of PEG 8 kDa in solution increased (Figure 6A), with apparent partitioning coefficients (K_{app}, calculated using fluorescence intensities inside and outside of the droplets) of 0.48 ± 0.04 at 2.5 wt.% PEG and 0.23 ± 0.08 at 20 wt.% PEG. Control experiments showing FITC alone accumulating inside coacervate droplets suggest that exclusion from the coacervate phase is based on interactions with PEG and not the fluorescent label **(Figure S6)**.

In contrast, TRITC-Ficoll 40 kDa was colocalized within the coacervate droplets, with an increase in partitioning behavior as wt.% Ficoll 70 kDa increased (Figure 6B), (K_{app} values of 1.9 ± 0.1 at 2.5 wt.% Ficoll and 3.1 ± 0.4 at 20 wt.% Ficoll). Given the wide variety of solutes that have been shown to accumulate in complex coacervates (e.g. small molecules,[13, 90-92] proteins,[92, 93] enzymes,[13, 91] nucleic acids,[14, 19, 94] polysaccharide-coated nanoparticles[13, 92]), the exclusion of PEG from the coacervate phase was initially surprising. Coacervate droplets have been found to contain less water than the surrounding supernatant phase, and thus provide a more hydrophobic environment.[13] Combined with PEG's strong affinity for binding water molecules,[95, 96] this provides a rationale for exclusion of PEG molecules from coacervate droplets, as there is more free water available in the supernatant phase. In fact, PEG is known to phase separate from some polyelectrolytes, for example producing distinct PEG-rich and DNA-rich phases at sufficiently high concentrations of double-stranded DNA.[97, 98]

Crowder partitioning data also provides insight into the temperature-dependent phase behavior discussed earlier. The significant difference between PEG's and Ficoll's impact on the T_C of polyU/spermine can be explained by the location of the crowding molecules during coacervation. The exclusion of PEG from polyU/spermine complexes could exert volume exclusion effects (that favor association/condensation) on the soluble polyU/spermine complexes, facilitating coacervate formation. This would account for the increased propensity for phase separation even before the loss of polyU secondary structure in the presence of PEG. Inclusion of Ficoll within polyU/spermine complexes accounts for the negligible impact of Ficoll on spermine required for coacervation and T_C.

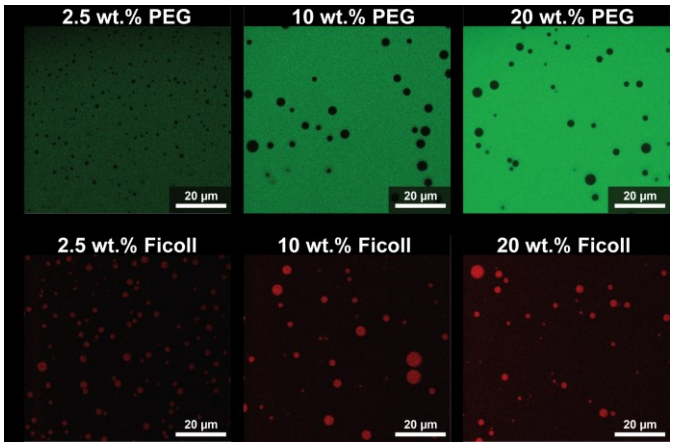

Figure 6: Confocal fluorescence microscope images illustrating partitioning of **(A)** fluorescently-labeled FITC-PEG 5 kDa and **(B)** fluorescently-labeled TRITC-Ficoll 40 kDa within a 0.05 wt.% polyU/0.5 wt.% spermine coacervate system. FITC-PEG is excluded from coacervate droplets, while TRITC-Ficoll partitions into the coacervate phase. Images were false-colored green (PEG) and red (Ficoll), and their brightness adjusted to aid in visualization. The brightness was adjusted by the same degree for all images of each crowder to conserve fluorescence trends.

The single-stranded oligonucleotide U15 RNA was chosen to probe the compartmentalization ability of polyU/spermine coacervates due to its limited interactions with polyU (as it does not form Watson Crick base pairs with polyU). Previous research has studied the partitioning behavior of oligonucleotides with varying base pairing affinities for polyU based on sequence.[14] Partitioning coefficients (K_{U15}), where K_{U15} = [U15 RNA concentration in the coacervate phase]/[U15 RNA concentration in the supernatant phase], were calculated to describe the partitioning behavior of Alexa 647-U15 RNA within the polyU/spermine coacervate system. Coacervate phase concentrations of U15 RNA were determined using confocal fluorescence microscopy, while supernatant phase concentrations were determined using bulk fluorescence measurements; both methods utilized standard curves generated from Alexa 647-U15 RNA in buffer. The K_{U15} in polyU/spermine coacervate droplets in the absence of crowder is in agreement with literature,[14] and a number of short oligonucleotides of RNA and DNA have been shown to partition into liquid droplets composed of the disordered region of Ddx4 protein with similar K values.[84] Increasing amounts of PEG significantly improved U15 RNA partitioning into the coacervate phase, with droplets formed in the presence of 20 wt.% PEG exhibiting a K_{U15} value 140x greater than that for droplets formed in the absence of crowder (Table 1, Figure 7B and D). Ficoll exhibited a less dramatic effect on U15 RNA partitioning, but 20 wt.% Ficoll still increased the K_{U15} value two-fold relative to droplets formed in dilute buffer (Table 1, Figure 7C-D). These findings demonstrate that the presence of crowding agents can substantially alter the localization of biomolecular solutes in complex coacervates. Increased accumulation of the RNA oligonucleotide was observed for both PEG, which was itself excluded, and for Ficoll, which was accumulated. The observed changes in RNA oligonucleotide partitioning result from alterations in microenvironments both within and outside the coacervate droplets, which may include changes in water activity and excluded volume, as well as the distribution/conformation of the coacervate-forming components. These crowding-induced changes in solute partitioning are important because even small changes in local biomolecule concentration could have substantial effects on intracellular processes.[99-101]

Finally, we used the U15 RNA partitioning data to investigate crowding-induced changes in phase volume. PEG has been shown to dehydrate precipitated and compressed polyelectrolyte complexes, leading to substantially decreased volume.[102] Although our samples are composed of different molecules and exist as liquid coacervates, dehydration by crowders such as PEG could help explain the observed partitioning behavior. As previously reported by Aumiller et al. for polyU/spermine in dilute solution,[14] the coacervate phase volume was calculated from the concentrations of U15 RNA in each phase, total moles of U15 RNA added, and total sample volume (eq S1). Calculated volumes suggest that crowding decreases the coacervate volume to a similar extent for both PEG and Ficoll (Table 1 and Figure S5). Addition of even a small amount of crowder (2.5 wt.% PEG or Ficoll) resulted in at least a two-fold decrease in the coacervate phase volume, from 1.2 µL in dilute buffer to 0.2 µL in 2.5 wt.% PEG and 0.5 µL in 2.5 wt.% Ficoll (data are statistically different at a 95% confidence level with p-values of 0.0002 and 0.005 respectively). The decreased coacervate phase

volume in the presence of crowders likely contributes to the increased partitioning of U15 RNA; this effect appears to be greater for PEG than for Ficoll, suggesting that PEG has a greater impact on the internal and/or external microenvironments as compared to Ficoll. While decreased phase volume at constant K can itself lead to increased local concentration for accumulated solutes,[103] here we also observed increased K_{RNA} as a consequence of crowding-induced changes in the coacervate and supernatant phase compositions.

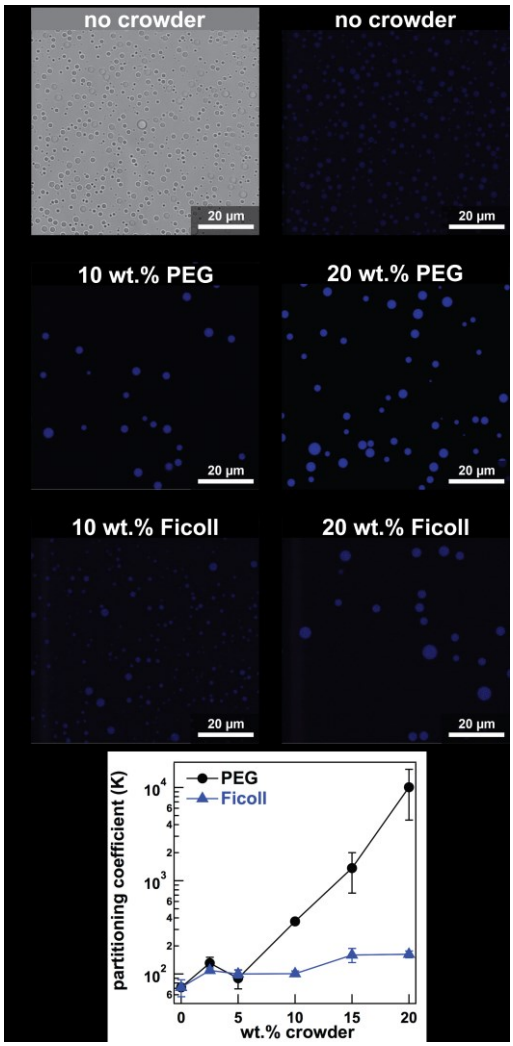

Figure 7: Confocal fluorescence images of Alexa 647-U15 RNA partitioning into 0.05 wt.% polyU/0.5 wt.% spermine coacervate droplets with **(A)** no crowder, **(B)** various amounts of PEG 8 kDa, and **(C)** various amounts of Ficoll 70 kDa. Images were false-colored and brightness was adjusted by the same degree for all images of each crowder to conserve fluorescence trends and aid visualization. **(D)** Partitioning coefficient (K) of U15 RNA as a function of wt.% crowder. Error bars take into account standard deviation between 10 measurements for coacervate phase concentration and triplicate measurements for supernatant phase concentration. Alexa 647-U15 RNA partitions into the coacervate phase in all cases, and partitioning increases with an increase in crowder, exhibiting more dramatic partitioning in PEG than in Ficoll.

Conclusions

This work explored the consequences of macromolecular crowding and cosolutes on the phase separation of polyU RNA and spermine by complex coacervation. Complex coacervation usually involves long, flexible polyelectrolytes (e.g., the polyU RNA used here, synthetic polyelectrolytes, or charge-rich IDP stretches). Therefore, in addition to the typical crowding-favored associations between molecules, individual long flexible molecules can undergo condensation in the presence of crowders, which could inhibit their association with binding partners by reducing the available contact area. Additionally, ion-pairing interactions that drive complex coacervation can be influenced by preferential interactions (i.e. chemical effects) of the crowders. In our experimental model system, the neutral macromolecular crowding agents PEG 8 kDa and Ficoll 70 kDa altered the phase behavior of polyU/spermine complex coacervation, emphasizing the importance of considering intracellular crowding when generating biomimetic models. Although previous studies suggested a loss in polyU base-stacking was necessary for phase separation,[14] here we observe that PEG promotes coacervation at temperatures lower than the observed T_m of polyU. PEG also promotes phase separation at lower spermine concentrations (and charge ratios). The complexity of these results illustrates the variety of ways in which crowders can impact the coacervation process, including the conformation of the coacervate-forming components, their interactions with other molecules, and their association to form a condensed phase.

Of particular interest were the results on crowder and RNA oligonucleotide distribution. Fluorescently labeled crowders exhibited different partitioning behavior, with PEG being excluded from coacervate droplets and Ficoll being accumulated. Despite their different partitioning, both PEG and Ficoll improved oligonucleotide accumulation into the coacervate droplets and decreased the total coacervate phase volume. These observations indicate that the presence of PEG or Ficoll altered the composition of the coacervate droplets and the external continuous phase, in part by reducing the internal water content. Since intracellular phase separation occurs under crowding conditions, our findings suggest that “background” macromolecules that do not directly participate in coacervation could nonetheless substantially influence solute distribution.

Table 1: Partitioning of Alexa 647-U15 RNA within polyU/spermine coacervates.

amount of crowding probe	Concentration added (μM)	coacervate phase concentration (μM)	supernatant phase concentration (μM)	partitioning coefficient (K_{U15})	coacervate phase volume (μL)
no crowder	0.2	10.8 ± 0.9	0.15 ± 0.03	72 ± 15	1.2 ± 0.7
2.5 wt.% PEG	0.2	23 ± 2	0.18 ± 0.02	130 ± 21	0.2 ± 0.2
5 wt.% PEG	0.2	17 ± 1	0.19 ± 0.04	90 ± 20	0.1 ± 0.6
10 wt.% PEG	0.2	72 ± 2	0.20 ± 0.01	370 ± 22	0.01 ± 0.03
15 wt.% PEG[a]	0.04[a]	19 ± 3[a]	0.014 ± 0.006[a]	1370 ± 629	0.4 ± 0.1
20 wt.% PEG[a]	0.04[a]	80 ±15[a]	0.008 ± 0.004[a]	10100 ± 5603	0.1 ± 0.02
2.5 wt.% Ficoll	0.2	17.7 ± 0.9	0.136 ± 0.007	109 ± 7	0.5 ± 0.1
5 wt.% Ficoll	0.2	17 ± 2	0.172 ± 0.006	100 ± 10	0.4 ± 0.1
10 wt.% Ficoll	0.2	19 ± 1	0.186 ± 0.007	101 ± 7	0.2 ± 0.1
15 wt.% Ficoll	0.2	28 ± 4	0.17 ± 0.01	160 ± 30	0.2 ± 0.1
20 wt.% Ficoll	0.2	29 ± 2	0.18 ± 0.01	163 ±13	0.2 ± 0.1

[a]Coacervate droplets in the presence of 15 and 20 wt.% PEG partitioned U15 RNA so strongly that fluorescence intensities were not accurately measurable; decreasing the concentration of added U15 RNA by a factor of 5 permitted fluorescence intensity measurement.

While the data presented here indicate the possibility of large crowder effects on coacervate formation and solute partitioning, they also underscore the differences between crowding agents. Inside living cells both the coacervate components and crowders will have greater chemical complexity, and preferential and repulsive interactions are likely to play a greater role than in the simple model system evaluated here. Important differences between in vitro and in vivo crowding experiments have been reported, with biomolecule identity and size appearing to play important roles in whether significant in vivo effects are observed. [22, 40, 58, 104, 105] For example, a FRET-based protein probe that exhibited crowding-induced compaction in synthetic polymer solutions did not compact in cell lysate or bacterial cell culture, while assembly of the bacterial cytoskeletal protein, FtsZ, into protofilament bundles was enhanced in both synthetic crowders and cell lysate.[58] To understand how intracellular crowding influences formation and properties of intracellular condensates formed by LLPS, it will be important for future studies to explore additional crowding agents, phase-separating systems, and biomolecular solutes.

Conflicts of interest

There are no conflicts to declare.

Acknowledgements

This work was supported by the National Science Foundation, grants MCB-1715984 and MCB-1244180. The authors thank Drs. Erica Frankel and Nathan Burrows for helpful discussions.

References

1. C. P. Brangwynne, T. J. Mitchison and A. A. Hyman, *Proc. Natl. Acad. Sci. U.S.A.*, 2011, **108**, 4334-4339.
2. C. P. Brangwynne, C. R. Eckmann, D. S. Courson, A. Rybarska, C. Hoege, J. Gharakhani, F. Jülicher and A. A. Hyman, *Science*, 2009, **324**, 1729-1732.
3. Timothy J. Nott, E. Petsalaki, P. Farber, D. Jervis, E. Fussner, A. Plochowietz, T. D. Craggs, David P. Bazett-Jones, T. Pawson, Julie D. Forman-Kay and Andrew J. Baldwin, *Mol. Cell*, 2015, **57**, 936-947.
4. J. Berry, S. C. Weber, N. Vaidya, M. Haataja and C. P. Brangwynne, *Proc. Natl. Acad. Sci. U.S.A.*, 2015, **112**, E5237-E5245.
5. S. Elbaum-Garfinkle, Y. Kim, K. Szczepaniak, C. C.-H. Chen, C. R. Eckmann, S. Myong and C. P. Brangwynne, *Proc. Natl. Acad. Sci. U.S.A.*, 2015, **112**, 7189-7194.
6. P. R. Banerjee, A. N. Milin, M. M. Moosa, P. L. Onuchic and A. A. Deniz, *Angew. Chem. Int. Ed.*, 2017, **56**, 11354–11359
7. Chi W. Pak, M. Kosno, Alex S. Holehouse, Shae B. Padrick, A. Mittal, R. Ali, Ali A. Yunus, David R. Liu, Rohit V. Pappu and Michael K. Rosen, *Mol. Cell*, 2016, **63**, 72-85.
8. M. Feric, N. Vaidya, Tyler S. Harmon, Diana M. Mitrea, L. Zhu, Tiffany M. Richardson, Richard W. Kriwacki, Rohit V. Pappu and Clifford P. Brangwynne, *Cell*, **165**, 1686-1697.
9. A. Molliex, J. Temirov, J. Lee, M. Coughlin, Anderson P. Kanagaraj, Hong J. Kim, T. Mittag and J. P. Taylor, *Cell*, 2015, **163**, 123-133.
10. A. A. Hyman, C. A. Weber and F. Jülicher, *Annu. Rev. Cell. Dev. Biol.*, 2014, **30**, 39-58.
11. Y. Shin and C. P. Brangwynne, *Science*, 2017, **357**.
12. C. P. Brangwynne, P. Tompa and R. V. Pappu, *Nat. Phys.*, 2015, **11**, 899-904.
13. S. Koga, D. S. Williams, A. W. Perriman and S. Mann, *Nat. Chem.*, 2011, **3**, 720-724.
14. W. M. Aumiller, F. Pir Cakmak, B. W. Davis and C. D. Keating, *Langmuir*, 2016, **32**, 10042-10053.
15. R. Chollakup, W. Smitthipong, C. D. Eisenbach and M. Tirrell, *Macromolecules*, 2010, **43**, 2518-2528.
16. D. Priftis and M. Tirrell, *Soft Matter*, 2012, **8**, 9396-9405.
17. S. Perry, Y. Li, D. Priftis, L. Leon and M. Tirrell, *Polymers*, 2014, **6**, 1756.
18. K. Kaibara, T. Okazaki, H. B. Bohidar and P. L. Dubin, *Biomacromolecules*, 2000, **1**, 100-107.
19. W. M. Aumiller Jr and C. D. Keating, *Nat. Chem.*, 2016, **8**, 129-137.
20. J. T. Wang, J. Smith, B.-C. Chen, H. Schmidt, D. Rasoloson, A. Paix, B. G. Lambrus, D. Calidas, E. Betzig and G. Seydoux, *eLife*, 2014, **3**, e04591.
21. A. Patel, Hyun O. Lee, L. Jawerth, S. Maharana, M. Jahnel, Marco Y. Hein, S. Stoynov, J. Mahamid, S. Saha, Titus M. Franzmann, A. Pozniakovski, I. Poser, N. Maghelli, Loic A. Royer, M. Weigert, Eugene W. Myers, S. Grill, D. Drechsel, Anthony A. Hyman and S. Alberti, *Cell*, **162**, 1066-1077.
22. M. Sarkar, A. E. Smith and G. J. Pielak, *Proc. Natl. Acad. Sci. U.S.A.*, 2013, **110**, 19342-19347.

23. H.-X. Zhou, G. N. Rivas and A. P. Minton, *Ann. Rev. Biophys.*, 2008, **37**, 375-397.
24. A. P. Minton, *Biopolymers*, 2013, **99**, 239-244.
25. R. J. Ellis, *Trends Biochem. Sci*, 2001, **26**, 597-604.
26. D. Hall and A. P. Minton, *Biochim. Biophys. Acta, Proteins Proteomics*, 2003, **1649**, 127-139.
27. P. D. Ross and A. P. Minton, *J. Mol. Biol.*, 1977, **112**, 437-452.
28. Y. Lin, D. S. W. Protter, M. K. Rosen and R. Parker, *Mol. Cell*, 2015, **60**, 208-219.
29. S. Ambadipudi, J. Biernat, D. Riedel, E. Mandelkow and M. Zweckstetter, *Nat. Commun.*, 2017, **8**, 275.
30. O. Annunziata, N. Asherie, A. Lomakin, J. Pande, O. Ogun and G. B. Benedek, *Proc. Natl. Acad. Sci. U.S.A.*, 2002, **99**, 14165-14170.
31. O. Annunziata, O. Ogun and G. B. Benedek, *Proc. Natl. Acad. Sci. U.S.A.*, 2003, **100**, 970-974.
32. R. W. Thompson, R. F. Latypov, Y. Wang, A. Lomakin, J. A. Meyer, S. Vunnum and G. B. Benedek, *J. Chem. Phys.*, 2016, **145**, 185101.
33. Y. Wang and O. Annunziata, *J. Phys. Chem. B*, 2007, **111**, 1222-1230.
34. R. Bhat and S. N. Timasheff, *Protein Sci.*, 1992, **1**, 1133-1143.
35. D. Kilburn, J. H. Roh, L. Guo, R. M. Briber and S. A. Woodson, *J. Am. Chem. Soc.*, 2010, **132**, 8690-8696.
36. D. Kilburn, R. Behrouzi, H.-T. Lee, K. Sarkar, R. M. Briber and S. A. Woodson, *Nucleic Acids Res.*, 2016, **44**, 9452-9461.
37. D. Kilburn, J. H. Roh, R. Behrouzi, R. M. Briber and S. A. Woodson, *J. Am. Chem. Soc.*, 2013, **135**, 10055-10063.
38. C. H. Spink and J. B. Chaires, *Biochemistry*, 1999, **38**, 496-508.
39. D. B. Knowles, A. S. LaCroix, N. F. Deines, I. Shkel and M. T. Record, *Proc. Natl. Acad. Sci. U.S.A.*, 2011, **108**, 12699-12704.
40. G. Rivas and A. P. Minton, *Trends Biochem. Sci*, 2016, **41**, 970-981.
41. C. A. Strulson, N. H. Yennawar, R. P. Rambo and P. C. Bevilacqua, *Biochemistry*, 2013, **52**, 8187-8197.
42. J. Ge, Sherry D. Bouriyaphone, Tamara A. Serebrennikova, Andrei V. Astashkin and Yuri E. Nesmelov, *Biophys. J.*, 2016, **111**, 178-184.
43. W. M. Aumiller, B. W. Davis and C. D. Keating, in *New models of the cell nucleus: Crowding, entropic forces, phase separation, and fractals*, eds. R. Hancock and K. Jeon, Academic Press, San Diego, CA, 2014, vol. 307, pp. 109-149.
44. S. F. Banani, A. M. Rice, W. B. Peeples, Y. Lin, S. Jain, R. Parker and M. K. Rosen, *Cell*, 2016, **166**, 651-663.
45. H. Zhang, S. Elbaum-Garfinkle, E. M. Langdon, N. Taylor, P. Occhipinti, Andrew A. Bridges, Clifford P. Brangwynne and Amy S. Gladfelter, *Mol. Cell*, **60**, 220-230.
46. C. Lee, H. Zhang, Amy E. Baker, P. Occhipinti, Mark E. Borsuk and Amy S. Gladfelter, *Dev. Cell*, 2013, **25**, 572-584.
47. C. S. Bond and A. H. Fox, *J. Cell Biol.*, 2009, **186**, 637.
48. S.-i. Nakano and N. Sugimoto, *Mol. BioSyst.*, 2017, **13**, 32-41.
49. V. B. Teif and K. Bohinc, *Prog. Biophys. Mol. Biol.*, 2011, **105**, 208-222.
50. A. Estévez-Torres and D. Baigl, *Soft Matter*, 2011, **7**, 6746-6756.
51. K. W. Leong, H. Q. Mao, V. L. Truong-Le, K. Roy, S. M. Walsh and J. T. August, *J. Controlled Release*, 1998, **53**, 183-193.
52. J. L. Santos, Y. Ren, J. Vandermark, M. M. Archang, J.-M. Williford, H.-W. Liu, J. Lee, T.-H. Wang and H.-Q. Mao, *Small*, 2016, **12**, 6214-6222.
53. S. Ristori, L. Ciani, G. Candiani, C. Battistini, A. Frati, I. Grillo and M. In, *Soft Matter*, 2012, **8**, 749-756.
54. K. Igarashi and K. Kashiwagi, *Int. J. Biochem. Cell Biol.*, 2010, **42**, 39-51.
55. A. E. Pegg, *IUBMB Life*, 2014, **66**, 8-18.
56. N. N. Deng and W. T. S. Huck, *Angew. Chem. Int. Ed.*, 2017, **56**, 9736-9740.
57. M. Z. Markarian and J. B. Schlenoff, *J. Phys. Chem. B*, 2010, **114**, 10620-10627.
58. J. Groen, D. Foschepoth, E. te Brinke, A. J. Boersma, H. Imamura, G. Rivas, H. A. Heus and W. T. S. Huck, *J. Am. Chem. Soc.*, 2015, **137**, 13041-13048.
59. B. Seed, in *Curr. Protoc. Immunol.*, John Wiley & Sons, Inc., 2001, DOI: 10.1002/0471142735.ima03ks21.
60. S. R. Gadagkar and G. B. Call, *J. Pharmacol. Toxicol. Methods*, 2015, **71**, 68-76.
61. E. A. Frankel, C. A. Strulson, C. D. Keating and P. C. Bevilacqua, *Biochemistry*, 2017, **56**, 2537-2548.
62. H. Motulsky and A. Christopoulos, *Fitting models to biological data using linear and non-linear regression: a practical guide to curve fitting*, GraphPad Software, Inc., San Diego, CA, 2003.
63. S. A. Frank, *Biol. Direct.*, 2013, **8**, 31-31.
64. L. Vitorazi, N. Ould-Moussa, S. Sekar, J. Fresnais, W. Loh, J. P. Chapel and J. F. Berret, *Soft Matter*, 2014, **10**, 9496-9505.
65. Q. Wang and J. B. Schlenoff, *Macromolecules*, 2014, **47**, 3108-3116.
66. S. Shahid, M. I. Hassan, A. Islam and F. Ahmad, *Biochim. Biophys. Acta*, 2017, **1861**, 178-197.
67. A. Christiansen, Q. Wang, A. Samiotakis, M. S. Cheung and P. Wittung-Stafshede, *Biochemistry*, 2010, **49**, 6519-6530.
68. J. Batra, K. Xu, S. Qin and H.-X. Zhou, *Biophys. J.*, 2009, **97**, 906-911.
69. D. B. Knowles, I. A. Shkel, N. M. Phan, M. Sternke, E. Lingeman, X. Cheng, L. Cheng, K. O'Connor and M. T. Record, *Biochemistry*, 2015, **54**, 3528-3542.
70. L. Sapir and D. Harries, *Curr. Opin. Colloid Interface Sci.*, 2015, **20**, 3-10.
71. M. Gao, D. Gnutt, A. Orban, B. Appel, F. Righetti, R. Winter, F. Narberhaus, S. Müller and S. Ebbinghaus, *Angew. Chem. Int. Ed.*, 2016, **55**, 3224-3228.
72. R. Harada, Y. Sugita and M. Feig, *J. Am. Chem. Soc.*, 2012, **134**, 4842-4849.
73. S.-i. Nakano and N. Sugimoto, *Biophys. Rev.*, 2016, **8**, 11-23.
74. L. Ninni, M. S. Camargo and A. J. A. Meirelles, *Thermochim. Acta*, 1999, **328**, 169-176.
75. J. R. Wenner and V. A. Bloomfield, *Biophys. J.*, 1999, **77**, 3234-3241.
76. S.-i. Nakano, D. Yamaguchi, H. Tateishi-Karimata, D. Miyoshi and N. Sugimoto, *Biophys. J.*, 2012, **102**, 2808-2817.
77. W. Szer, *Ann. N. Y. Acad. Sci.*, 1970, **171**, 801-809.

78. A. M. Michelson, *Biochim. Biophys. Acta*, 1962, **55**, 841-848.
79. J. R. Fresco, *Trans. N. Y. Acad. Sci.*, 1959, **21**, 653-658.
80. J. C. Thrierr, M. Dourlent and M. Leng, *J. Mol. Biol.*, 1971, **58**, 815-830.
81. M. N. Lipsett, *Proc. Natl. Acad. Sci. U.S.A.*, 1960, **46**, 445-446.
82. N. F. Dupuis, E. D. Holmstrom and D. J. Nesbitt, *Proc. Natl. Acad. Sci. U.S.A.*, 2014, **111**, 8464-8469.
83. Y. Liu, F. Kermanpour, H. L. Liu, Y. Hu, Y. Z. Shang, S. I. Sandler and J. W. Jiang, *J. Phys. Chem. B*, 2010, **114**, 9905-9911.
84. T. J. Nott, T. D. Craggs and A. J. Baldwin, *Nat. Chem.*, 2016, **8**, 569.
85. P. Anderson and N. Kedersha, *Nat. Rev. Mol. Cell Biol.*, 2009, **10**, 430-436.
86. M. Kato, T. W. Han, S. Xie, K. Shi, X. Du, L. C. Wu, H. Mirzaei, E. J. Goldsmith, J. Longgood, J. Pei, N. V. Grishin, D. E. Frantz, J. W. Schneider, S. Chen, L. Li, M. R. Sawaya, D. Eisenberg, R. Tycko and S. L. McKnight, *Cell*, 2012, **149**, 753-767.
87. T. W. Han, M. Kato, S. Xie, L. C. Wu, H. Mirzaei, J. Pei, M. Chen, Y. Xie, J. Allen, G. Xiao and S. L. McKnight, *Cell*, 2012, **149**, 768-779.
88. A. Aguzzi and M. Altmeyer, *Trends Cell Biol.*, **26**, 547-558.
89. R. Roodbeen and J. C. M. van Hest, *Bioessays*, 2009, **31**, 1299-1308.
90. J. P. Swanson, L. R. Monteleone, F. Haso, P. J. Costanzo, T. Liu and A. Joy, *Macromolecules*, 2015, **48**, 3834-3842.
91. L. Tian, N. Martin, P. G. Bassindale, A. J. Patil, M. Li, A. Barnes, B. W. Drinkwater and S. Mann, *Nat. Commun.*, 2016, **7**, 13068.
92. D. S. Williams, S. Koga, C. R. C. Hak, A. Majrekar, A. J. Patil, A. W. Perriman and S. Mann, *Soft Matter*, 2012, **8**, 6004-6014.
93. K. A. Black, D. Priftis, S. L. Perry, J. Yip, W. Y. Byun and M. Tirrell, *ACS Macro Lett.*, 2014, **3**, 1088-1091.
94. E. A. Frankel, P. C. Bevilacqua and C. D. Keating, *Langmuir*, 2016, **32**, 2041-2049.
95. S. L. Hager and T. B. Macrury, *J. Appl. Polym. Sci.*, 1980, **25**, 1559-1571.
96. J. Israelachvili, *Proc. Natl. Acad. Sci. U.S.A.*, 1997, **94**, 8378-8379.
97. B. Monterroso, S. Zorrilla, M. Sobrinos-Sanguino, C. D. Keating and G. Rivas, *Sci. Rep.*, 2016, **6**, 35140.
98. N. Biswas, M. Ichikawa, A. Datta, Y. T. Sato, M. Yanagisawa and K. Yoshikawa, *Chem. Phys. Lett.*, 2012, **539-540**, 157-162.
99. J. E. Ferrell and E. M. Machleder, *Science*, 1998, **280**, 895-898.
100. J. E. Ferrell and S. H. Ha, *Trends Biochem. Sci*, 2014, **39**, 496-503.
101. D. Koshland, A. Goldbeter and J. Stock, *Science*, 1982, **217**, 220-225.
102. H. H. Hariri, A. M. Lehaf and J. B. Schlenoff, *Macromolecules*, 2012, **45**, 9364-9372.
103. C. A. Strulson, R. C. Molden, C. D. Keating and P. C. Bevilacqua, *Nat. Chem.*, 2012, **4**, 941-946.
104. A. H. Elcock, *Curr. Opin. Struct. Biol.*, 2010, **20**, 196-206.
105. A. J. Wirth and M. Gruebele, *Bioessays*, 2013, **35**, 984-993.

1